Spatial distribution of fallout and lithogenic radionuclides controlled by soil carbon and water erosion in an agroforestry South-Pyrenean catchment

Leticia Gaspar [a,*], **Ivan Lizaga** [a], **Ana Navas** [a]

[a] *Soil and Water Department, Estación Experimental de Aula Dei (EEAD-CSIC), Zaragoza, Spain*

Corresponding Author: leticia.gaspar.ferrer@gmail.com (Gaspar, L)

Graphical Abstract

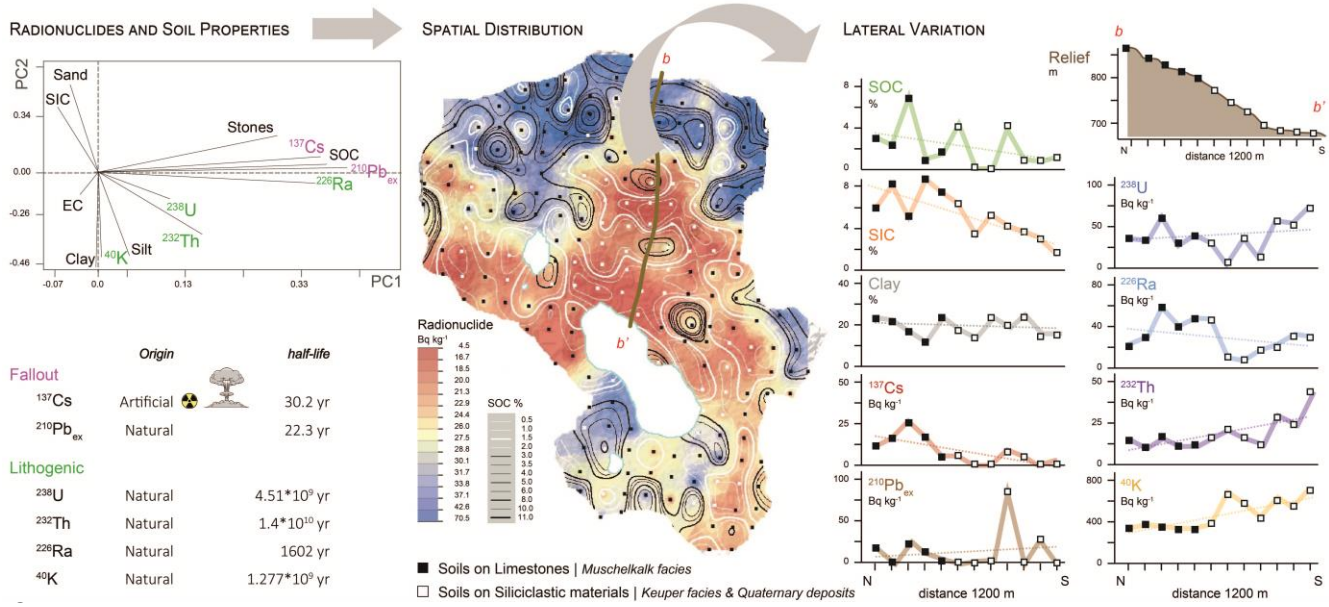

Highlights

- Spatial patterns of radionuclides depend on parent materials and soil processes.
- Strong links of ^{137}Cs and $^{210}P_{ex}$ to SOC indicate their efficient fixation in soils.
- ^{232}Th, ^{40}K, ^{226}Ra and ^{238}U activities result from minerals in clay and silt particles.
- Erosion plays a key role in mobilising and redistributing fallout radionuclides.
- Lithogenic radionuclides are sensitive to physical processes in high soil loss areas.

Abstract

The mineral composition of soils and weathering processes are known to control the natural radioactivity of soils but research on the influence of water erosion and of main soil properties in the spatial variability of lithogenic and fallout radionuclides remains little investigated in heterogeneous agroecosystems with complex landscape. An extensive study was conducted to determine the mass activities of fallout (^{137}Cs, ^{210}Pb$_{ex}$) and lithogenic radionuclides (^{238}U, ^{226}Ra, ^{232}Th, ^{40}K) an assess the main controls affecting their spatial variations in a representative 2.5 km^2 Pre-Pyrenean catchment of north-eastern Spain. The complex agroforestry catchment holds two distinctive parent materials, Muschelkalk limestones and Keuper argillaceous marls, in which the variability of the main soil properties and soil erosion patterns are well characterised. A total of 228 soil samples have been measured by using a high-purity germanium detector. Lithological influence on the variability of radionuclides was investigated and our results indicate that there are strong significant differences between the mass activities of ^{137}Cs, ^{210}Pb^{ex}, ^{226}Ra and ^{40}K based on the two different parent materials. Positive correlations were found among the radioactivity contents of ^{232}Th and ^{40}K and the clay content. Total organic carbon (SOC) was also positively correlated with ^{137}Cs, ^{210}Pbex and ^{226}Ra activities, whereas carbonate content and SIC were negatively correlated with the radionuclides with higher significance in soils on limestones.

To gain knowledge on the spatial variability of the radionuclides within the landscape, maps of the distribution of radionuclides were generated by GIS interpolation tools of the entire set of measured activities and soil properties within a 100 x 100 m grid. The spatial patterns obtained, besides the variations of radionuclides along four selected transects, confirm the key role of water erosion in the mobilisation of fallout radionuclides, especially ^{137}Cs, while lithogenic radionuclides were sensitive to physical

processes in areas where soil loss was intense. This study not only filled the gap of radioactivity data in agroforestry systems with contrasting parent materials, but also shed light on the potential of radionuclides for tracking soil redistribution processes in fingerprints studies.

Keywords: ^{137}Cs, $^{210}Pb_{ex}$, ^{238}U, ^{226}Ra, ^{232}Th, ^{40}K; Gamma spectrometry; SOC; SIC; Parent material; Soil redistribution.

1. Introduction

Naturally occurring radioisotopes (NOR) are the main sources of gamma radiation in rocks and soils at levels that are of no concern to human health or the environment (Elless and Lee, 2002). Natural radioactivity mainly consists of U-238 and Th-232 series, their decay products and ^{40}K, characterised by a long half-life period. A significant amount of man-made radionuclides like ^{137}Cs as a result of nuclear weapon tests and nuclear accidents also contributes to the radioactive flux. In addition to the anthropogenic radionuclides, fallout radionuclides comprise NOR released from the Earth's surface like $^{210}Pb_{ex}$ or generated by interactions of cosmic radiation with atmospheric components (^{7}Be).

Natural environmental radioactivity of soils depends primarily on geological and geographical conditions, and is controlled by the mineral composition of parent materials (Shender, 1997), but physico-chemical properties of soils play a major role in the mobility and bioavailability of the environmental radionuclides in the ecosystem (Kabata-Pendias, 2011). In addition, fallout radionuclides $^{210}Pb_{ex}$ and ^{137}Cs are distributed in the landscapes by physical processes because of its rapid and strong adsorption onto fine soil particles after its fallout and subsequent mobilization by soil erosion. Fallout radionuclides fixed

by clay and organic matter are transferred in the agroecosystems associated to soil movement what has been effectively used to trace soil redistribution during the last decades (e.g. Mabit et al., 2008; Walling, 2012; Gaspar et al., 2013; Navas et al., 2014).

When soil erosion occurs, the surface layer and low-density proportions of soil, such as soil organic carbon (SOC), are preferentially removed by runoff, wind, and/or tillage activities (Lal, 2003). Topography coupled with geomorphic processes can significantly influence the dynamics of soil redistribution processes that play an important role in the mobilization and spatial distribution of physicochemical properties and the elemental composition of soils, affecting the distribution pattern of both natural and anthropogenic radionuclides.

The interactions between radionuclide and the soil include physical (reversible) sorption governed by the uncompensated charges on the surface of the soil particles, and the chemical (principally irreversible) sorption through high affinity, specific interactions, and establishment of covalent bonds (Sposito, 2008). A capacity of the soil itself to immobilize radionuclides is the main factor controlling activity concentrations available to biota, and it operates in conjunction with numerous external factors. Due to the finest particle size, clay minerals exhibit the largest surface area, important for soil chemistry and CEC, but also for water holding capacity important for transporting nutrients and pollutants to soil organisms and plants. In addition, soil organic matter significantly contributes to the soil CEC and to the water holding capacity.

Soil texture and structure, mineral composition, organic components, redox potential and pH, as well as rainfall, climate changes, and soil management, are recognized as important for radionuclide mobility (Iurian et al., 2015). The pH of the soil, cation exchange capacity (CEC), and soil organic carbon (SOC) are the physicochemical

characteristics most often correlated with the distribution of the radionuclides (Navas et al., 2011; Smičiklas et al., 2015).

Concerning the environmental applications of radionuclides the potential for using fallout radionuclides to provide soil redistribution rates and to age-date sediments have been clearly demonstrated in many different areas of the world (e.g. Ritchie and McHenry, 1990; Navas et al., 2014; Yao and Xue, 2016; Mabit et al., 2018). Furthermore, distinctive concentrations of radionuclides relate to geological and morphological features of specific locations and soil in these locations will contain unique nuclide concentrations that relate to its source. In the last decades, both fallout and lithogenic radionuclides have been used as tracers in fingerprinting studies to effectively discriminate sediment sources and to understand and quantify the sediment provenance (e.g. Motha et al., 2003; Palazón et al., 2015; Owens et al., 2016; Lizaga et al., 2020). Previous studies confirm the potential of using lithogenic radionuclides to identify different sedimentary rocks with contrasted lithologies (de Jong et al., 1994), and recently, Navas et al. (2020) effectively discriminated source of sediments in Aldegonda Glacier (Svalbard) based on differences of parent materials.

It has long been recognized that the mineral composition of the parent material and the extent of weathering and leaching largely control the radioactivity of soils (Graham, 1964), however little is known on the effect of soil erosion on the distribution of lithogenic radionuclides. In this regard is of relevance to acquire information on the processes involved in the mobility and the spatial distribution of radionuclides to what it is necessary to gain knowledge on the behaviour of both fallout and lithogenic radionuclides in a variety of environments. Thus detailed information on specific soil characteristics, soil redistribution patterns and land use in different climatic regions with

various geological substrates, may be helpful to better characterise radionuclide behaviour in soil.

We hypothesize that the soil composition including soil organic and inorganic carbon and grain size fractions with differences in the sorption to mineral soil constituents might represent important factors controlling the radionuclides in soil. On the other hand physiographic factors driving runoff and water pathways, soil redistribution processes (erosion/deposition) and land uses could also affect the mobilization and transfer of radionuclides in soils.

Our research aims to fill the gap of knowledge related to the spatial distribution of radionuclides with main soil properties and soil processes in complex agroforestry landscapes. The novelty of this study lies in assessing the main controls influencing the behaviour of radionuclides in soils developed on sedimentary rocks , in which the stable elemental distributions have already been found to be primarily controlled by parent material (Gaspar et al., 2020a).

To this end we establish a comprehensive sampling design in an agroforestry catchment to collect soil samples spatially distributed over two dominant lithologies in the Southern Pyrenean region. We analyse the activities of fallout and lithogenic radionuclides in bulk soil cores using HPGe gamma ray spectrometer to examine the relations with soil organic and inorganic carbon and main soil properties under different land uses and soil conservation conditions. This study is aimed to determine the spatial distribution of ^{137}Cs, $^{210}Pb_{ex}$ as well as the primordial natural radionuclides ^{238}U, ^{226}Ra, ^{232}Th and ^{40}K to evaluate which factors are controlling the distribution of radionuclides in function of the different parent materials, and to assess the influence of soil redistribution processes on the variability of the fallout and lithogenic radionuclides. Our findings will provide insights on the influencing factors driving the variations of

141 radionuclides in mountain Mediterranean landscapes, where a variety of land uses and an
142 abrupt topography plays a key role in soil redistribution.
143
144 **2. Material and Methods**
145 *2.1 Study area*
146 The study was carried out in the endorheic Estaña catchment, located in the central
147 sector of the outer ranges of the Spanish Pyrenees (Fig. 1). This is a karst area holding
148 two small lakes in the lower part of the catchment characterised by abrupt topography
149 and a complex mosaic of land uses. Information of the topographic features derived from
150 a detailed DEM and the drainage system in the catchment is well-described from previous
151 studies (Gaspar and Navas, 2013; Navas et al., 2013, 2014; Gaspar et al., 2019), including
152 the relationship between topographic attributes and soil and carbon mobilization (Gaspar
153 et al., 2020b). Gentle slopes predominate in the south part of the catchment and
154 surrounding the lakes, while steep slopes (> 15%) are most common and occupy nearly
155 45% of the catchment. The climate is Mediterranean continental type with a mean annual
156 rainfall of ca. 595 mm.
157 The underlying materials consist mainly of gypsiferous marls, dolomites, and
158 limestones of the Mesozoic and Neogene ages, besides some Quaternary deposits. The
159 soils developed on limestones are mainly Calcisols and Leptosols, covering 32 and 30%
160 of the total surface of the catchment, while soils on siliciclastic materials are mainly
161 Regosols, Calcisols and Gypsisols developed on the gypsiferous outcrops.
162 Based on the parent materials, soil samples were grouped into limestones and
163 siliciclastic materials. Soils on limestones correspond to Muschelkalk facies, which make
164 up the higher reliefs and occupy the highest elevation and steeper slopes. The siliciclastic
165 materials are composed of low-permeability marls and claystone formation (Keuper

166 facies), besides Quaternary soils. The gypsiferous marls occupy mainly flat areas
167 surrounding the lakes and also some steep slopes, which are under cultivation.
168
169 *2.2 Sampling design and laboratory analysis*
170 A total of 228 bulk soil cores were collected at the intersection points within a 100 x
171 100 m grid (Fig. 1). The soils were sampled by using 8 cm diameter core driller, until
172 obtaining the total useful depth of the soil profile that vary in function of soil types
173 between 15 to 45 cm depth. Furthermore, on the grid points,4 transects were established
174 (Fig. 1), from the divides of the catchment to the bottom part of the slope until the edge
175 of the Estaña lake. Two transects were selected as a mixture of soils on limestones and
176 siliciclastic materials (a-a' and b-b'), while the other two transects were selected to
177 characterize a slope with homogeneous soils only on limestones (c-c' and d-d').
178 In the laboratory, soil samples were air-dried, ground, homogenized, and quartered,
179 before being passed through a 2-mm sieve. The coarse fraction (stones) corresponds to
180 particles above 2 mm and was separated from the fine fraction (<2 mm) that was used for
181 general soil properties analysis. Analyses included main soil properties and mass
182 activities of fallout radionuclides (FRNs: ^{137}Cs,$^{210}Pb_{ex}$) and the lithogenic radionuclides
183 (^{238}U, ^{232}Th, ^{40}K, ^{226}Ra) for the 150 and 78 soil samples on limestones and siliciclastic
184 materials, respectively.
185 Radionuclide activity in the soil samples was measured using a Canberra high
186 resolution, low background, low energy, hyperpure coaxial germanium detector (XtRa
187 GX3019, Meriden, USA) coupled to an amplifier and multichannel analyzer, using Genie
188 2000 software and calibrated by using certified samples in the same geometry of the study
189 samples. The detector had an efficiency of 50%, and a 1.92 keV resolution (shielded to
190 reduce background) and was calibrated using standard certified samples with the same

geometry as the measured samples. Subsamples of 50 g were loaded into plastic containers.

Gamma emissions of ^{238}U, ^{232}Th, ^{40}K, ^{226}Ra, ^{137}Cs and $^{210}Pb_{ex}$ (in Bq kg^{-1} air-dry soil) were measured considering the appropriate corrections for laboratory background, ^{238}U was determined from the 63-keV line of ^{234}Th (LLD: 2.6 Bq kg^{-1}), ^{232}Th was estimated using the 911-keV photopeak of ^{228}Ac (LLD: 0.5 Bq kg^{-1}), ^{40}K from the 1461 keV photopeak (LLD: 2 Bq kg^{-1}), ^{226}Ra was determined from the 352-keV line of ^{214}Pb (LLD: 0.5 Bq kg^{-1}) (Van Cleef, 1994), and ^{137}Cs activity was determined from the 661.6 keV photopeak (LLD: 0.4 Bq kg^{-1}). The $^{210}Pb_{ex}$ activities, which correspond with the upward diffusion of ^{222}Rn in the atmosphere, were estimated from the difference between the total ^{210}Pb (LLD: 3.5 Bq kg^{-1}) (47 keV photopeak) activity and the ^{226}Ra activity, measured a month after the samples were sealed, which ensured a secular equilibrium between ^{222}Rn and ^{226}Ra. Count times over 24 h provided an analytical precision of the measurements at the 95% level of confidence that ranged from ±3% to 10%.

Soil organic carbon (SOC) was determined by the dry combustion method using a LECO RC-612 multiphase carbon analyser. Calcium carbonates were measured using a Barahona pressure calcimeter, and the percentage of soil inorganic carbon (SIC) was estimated from stoichiometry. Granulometric analyses were done to determine the soil texture and obtain the contents of clay, silt and sand fractions by using laser equipment. Other properties such as pH and electrical conductivity (EC) were analysed according to standard procedures.

2.3 Data Analysis

Lithological information of the sampling sites was extracted from the National Geological Map (1:50,000_MAGNA) (IGME, info.igme.es/cartografiadigital),

validating each sampling point with the physical and chemical properties analysed in the soils besides the observations in situ during several field campaigns.

Analysis of variance was used to assess the statistical significance of the differences in the means (ANOVA test) and medians (Kruskal-Wallis test) of the radionuclide activities and soil properties at a *p-value* ≤ 0.05 using Least Significant Difference. Correlation coefficients were used to assess the relationships between the radionuclides and the main soil properties. Discriminant function analyses (DFA) were performed to assess if the radionuclides and soil properties differentiated the two types of parent materials in the study area, while principal component analyses (PCA) were performed to assess the links between soil properties and radionuclides in the soils on limestones and siliciclastic materials. Finally, the multiple regressions models between radionuclides and soil properties were derived using a step-wise methodology, and GLM models were conducted to include categorical factors.

Spline interpolator method (ArcGIS 10.4), which fits a minimum curvature surface through the input points, was used to represent the spatial distribution of the radionuclides activities and soil properties, including the isolevels of the SOC, SIC and clay content within the catchment. To evaluate the lateral mobilisation and availability of radionuclides in soils the mass activity versus slope distance along the 4 transects selected were plotted.

Soil redistribution rates estimated after conversion of ^{137}Cs measurements (Soto and Navas, 2004, 2008) for the soil samples and the derived maps of the spatial distribution of soil erosion and deposition rates for two sub-catchments of the study catchment are available from previous research (Navas et al., 2013, 2014). These studies reported large variability of soil redistribution rates with mean values of soil erosion and deposition of 20 and 12 Mg ha^{-1} year^{-1}, respectively.

241

242 **3. Results**

243 *3.1 Factors affecting the radionuclides in soils*

244 The soils are stony with a moderately alkaline pH (mean: 8.04), low electric
245 conductivity, and the grain size distributions showed a predominance of silt fraction (silt
246 loam texture) (Table 1). The content of SOC and SIC varied from almost negligible values
247 to reaching 10 and 11%, respectively, while the carbonate contents were highly variable
248 ranging between 3 and 86%. The median values of the mass activities of ^{137}Cs and $^{210}Pb_{ex}$
249 were 8 and 9.3 Bq kg^{-1}, while that of the lithogenic radionuclides ^{238}U, ^{226}Ra, ^{232}Th, and
250 ^{40}K were 46, 25, 23 and 445 Bq kg^{-1}, respectively, falling within the reported world
251 averages for areas of normal radioactivity and with a dominance of ^{40}K over the rest of
252 radionuclides (Table 1).

253 Most radionuclides and soil properties showed significant differences (*p-value*
254 ≤0.05) related to the parent material, between soils on limestones and those on siliciclastic
255 materials (Table 2). The mass activity of ^{137}Cs and $^{210}Pb_{ex}$, as well as ^{226}Ra and ^{40}K,
256 differed significantly among the soils. In contrast, neither the mean (ANOVA) nor the
257 median (KW analysis) mass activities of ^{238}U and ^{232}Th were significantly different. Soils
258 on limestones showed significantly higher ^{137}Cs, $^{210}Pb_{ex}$ and ^{226}Ra mass activities than
259 soils on siliciclastic materials, besides slightly higher means of ^{238}U and ^{232}Th were
260 observed. Conversely, ^{40}K was significantly higher in soils on siliciclastic materials than
261 on limestones, recording the highest mass activities in soil. Significant differences were
262 also observed for the main soil properties. The means of SOC, SIC, carbonate and stones
263 contents were significantly higher in soils on limestones with slightly higher sand content,
264 while soils on siliciclastic materials of Keuper recorded significantly higher values of EC
265 and slightly higher silt content (Table 2).

The radionuclides were, in general, positively correlated with each other. The ^{137}Cs and $^{210}Pb_{ex}$ were positively and significantly correlated (r=0.46, *p-value* ≤0.05), especially for soils on siliciclastic materials (r=0.60). Similarly, ^{137}Cs mass activities were positively and significantly correlated with ^{226}Ra (r=0.60), which showed a relatively weaker correlation with $^{210}Pb_{ex}$ (r=0.30). The relationships between the fallout and lithogenic radionuclides were positive but with low *Pearson's* correlation coefficients (< 0.02 for ^{137}Cs and < 0.01 for $^{210}Pb_{ex}$). Regarding the correlations between the lithogenic radionuclides, ^{232}Th was positively and strongly correlated with ^{40}K (r=0.66) and ^{226}Ra (r=0.43). However, the ^{238}U showed a weak correlation with ^{226}Ra (r=0.36) and an absence of correlation with ^{232}Th and ^{40}K.

Concerning the relationships between radionuclides and main soil properties (Table 3), the SOC content was significantly and positively correlated with the fallout radionuclides, especially with ^{137}Cs (r=0.81). Correlations between SOC and lithogenic radionuclides were moderate for ^{226}Ra and ^{232}Th, and no correlations were found for ^{40}K and ^{238}U. In contrast, SIC content was negatively correlated with the abundance of each of the lithogenic and fallout radionuclides, especially with ^{40}K and ^{232}Th, which reached *Pearson's* correlation coefficients of up to 0.70 in soils on limestones. The clay content was only positively correlated with the mass activity of ^{40}K and ^{232}Th in soil on limestones although the correlations were moderate (r= 0.4 and 0.3, respectively), while no correlations of clay with ^{137}Cs and $^{210}Pb_{ex}$ were observed. Remarkably, the mass activities of all lithogenic radionuclides were positively correlated with sand and negatively correlated with the silt fraction for soils on siliciclastic materials (Table 3). The values of natural radionuclides (^{40}K, ^{238}U, ^{226}Ra, ^{232}Th) activities did not show a clear trend in relation to altitude, curvature and steepness. Only ^{137}Cs mass activities were weak to moderately correlated with the slope gradient (r= 0.3) and with the altitude (r= 0.5).

The main soil properties and the content of fallout and lithogenic radionuclides were used for the linear discriminant analysis (LDA) shown in Figure 2. The scatter plot of all samples showed clear discrimination between soils on limestones and on siliciclastic materials, with 82.9% of the cases correctly classified. Still, an overlap was observed for some samples between the two groups of soils. The principal component analysis (PCA) indicated that combinations of all variables explained a relatively high proportion of the total variation between the samples. Four components, with eigenvalues higher than 1, explained 73% of the total variance. The scatter plot between components PC1 and PC2 (Fig. 3), which accounted for more than 50% of the total variance, successfully discriminated between variables. On one side, the fallout radionuclides (^{137}Cs and ^{210}Pb$_{ex}$), SOC content and ^{226}Ra included in PC1 explained 29% of the total variance. ^{238}U, ^{232}Th, ^{40}K, together with the fine fractions (silt and clay content) and EC were clustered in PC2 that explained 21% of the total variance and were inversely related with the SIC and sand contents.

The step-wise linear regression analyses summarised in Table 4 indicated that nearly 60% of the variation of the ^{137}Cs mass activity was explained by the contents of SOC, stoniness and silt fraction, while in the case of ^{210}Pb$_{ex}$, SOC content only explained around 20% of the total variance (Table 4). For ^{226}Ra and ^{232}Th, the regression models only explained 38% and 42% of the total variation, respectively, mainly due to the content of SOC and SIC. For ^{40}K, the SIC content was the main explanatory factor and together with stoniness, clay and EC explained nearly 50% of the variance, while the SOC content was of lesser importance. A satisfactory model could not be found to explain the variability of ^{238}U, suggesting high complexity in the behaviour of this radionuclide. The regression models performed for soils on siliciclastic materials explained higher percentages of the total variance of ^{137}Cs, ^{210}Pb$_{ex}$ and ^{226}Ra than the previous models, increasing the results

316 by 8, 14 and 13 %, respectively, while the highest percentages of explanation of the total
317 variance for ^{232}Th and ^{40}K were obtained in soils on limestones (increasing by 20 and 6%,
318 respectively, the previous models) (Table 4).

319 Significantly higher mass activities of ^{137}Cs, ^{210}Pb$_{ex}$, ^{226}Ra and ^{232}Th, besides slightly
320 higher ^{40}K and ^{238}U, were found to be coincident with previously identified deposition
321 sites in the study area (Navas et al., 2013, 2014; Gaspar et al., 2019). Regarding land uses,
322 soils that had natural vegetation cover registered significantly higher content of ^{137}Cs,
323 ^{210}Pb$_{ex}$ and ^{226}Ra but significantly lower content of ^{40}K. Similar contents of ^{232}Th and ^{238}U
324 were found in uncultivated and cultivated soils.

325 Despite the above results, the GLM models developed to include these factors along
326 with the soil properties, only improved the results for ^{137}Cs. Soil redistribution, SOC and
327 silt contents explained 74% of the total variance of ^{137}Cs, compared to the 54% explained
328 by the step-wise regression analysis. For the rest of the radionuclides, the GLM models
329 did not significantly improved the results, with slight increases in the explanation of the
330 variances (between 1 and 2%) compared to the regression models in Table 4.

331

332 *3.2 Spatial distribution of the radionuclides*

333 The maps of the mass activities of ^{137}Cs and ^{210}Pb$_{ex}$ were quite coincidental and
334 exhibited similar spatial distributions, with the highest activities recorded in the northern
335 third of the catchment and the southwest area (Fig. 4). Nevertheless, differences were
336 found in areas located in the east side and in the southeast part, where ^{210}Pb$_{ex}$ activities
337 increased while ^{137}Cs activities were relatively lower. The overlay of the isolevels of SOC
338 over the fallout radionuclides revealed strong coincidences in their spatial distribution
339 (Fig. 4). The highest mass activities were on the areas with the highest SOC contents,
340 especially for ^{137}Cs. Clay isolevels did not exhibited coincidental distributions with that

of the fallout radionuclides and patterns were quite unspecific. In that way, the highest contents of clay fractions were recorded in areas with low mass activities but also low contents of clay were found in these areas as well as in others with high activities. The highest contents of sand were mostly found in areas with low activities of ^{137}Cs and $^{210}Pb_{ex}$, but also in areas of high activities. Considering the soil redistribution patterns previously established, the lowest activities of the fallout radionuclides were found on the steepest areas with less vegetation cover were the eroded areas were identified (Navas et al., 2013, 2014).

The spatial distribution of ^{40}K, ^{226}Ra, ^{232}Th and ^{238}U displayed different patterns (Fig. 5). The distribution of ^{226}Ra exhibited some similarities with the distribution of the fallout radionuclides, although most of the differences were identified in the southern part of the catchment. Something similar occurred with the distribution of ^{232}Th, but the similarities with the fallout radionuclides were less evident than with ^{226}Ra. It was also noticed that ^{232}Th reached high activities along the entire eastern edge of the catchment divide, which were highly coincidental with relatively high values of clay and low of sand. Similarly, low contents of clay matched with low activities of ^{226}Ra and ^{232}Th. In the case of ^{40}K, a practically opposite distribution to that of carbonate content was observed and both the highest and the lowest activities of ^{40}K were recorded in areas with high SOC values. In some areas, located in the north-eastern part of the catchment, high coincidence was observed between ^{40}K and clay and EC values, however, in other areas under agricultural use these patterns were the opposite. Remarkable, the lack of coincidence between ^{40}K and SOC, and the very low values of ^{40}K recorded in the south-eastern part of the catchment. The distribution map of ^{238}U was highly variable and unspecific as patterns were not coincidental with any of the soil properties or other radionuclides.

Fig 6 shows how the radionuclides and some soil properties vary along the slope for each of the four selected transects. Overall, transects a–a' and b–b', which are composed by a mix of soils on limestones and siliciclastic materials, showed larger variability of the radionuclides and soil properties. In these transects, data dispersion respect to the general linear trend along the slope was greater than in transects c and d, which are composed only of limestones. As showed by the trendlines along transects c–c' and d–d', more homogeneous patterns were observed for soil properties and radionuclides activities.

In terms of similarity trends, the contents of SOC and ^{137}Cs were quite coincidental in the four transects, with higher contents at the upper of the slope and lower contents at the bottom part. In the mixed transects, from position 6 to downslope, which corresponds with siliciclastic materials, a pattern of enrichment of lithogenic while depletion of fallout radionuclides was found. A different pattern was observed for transect c, where all radionuclides tended to decrease along the steep slope over limestones, showing a good parallelism with SOC but opposite to SIC content. On the other hand, in transect d, which is characterized by a gentle slope, more discrepancies between lithogenic radionuclides were observed, with depleted levels of ^{226}Ra and ^{40}K and enrichment of ^{238}U and ^{232}Th.

4. Discussion

4.1 Factors affecting the radionuclides in soils

Radionuclide mass activities in the study soils differ as a function of the parent material. Whereas DFA results indicate good discrimination between both parent materials, there was some overlap for 13% of samples incorrectly classified (Fig. 2). This could be explained by the complex tectonic and the derived geomorphological characteristics which are important to consider when interpreting the lithological information in soil samples of these areas. In addition, it should be also considered that

siliciclastic soils include not only Keuper facies but also Quaternary deposits, which could produce certain variability.

In general, the mean radioactivity levels of lithogenic and fallout radionuclides are similar to the world average concentrations for sedimentary rocks (UNESCAR, 2000). The radionuclide contents are also consistent with records found in soils developed on the Tertiary Flysch in the southern central Pyrenees (Navas et al., 2002b). Some differences in the content of lithogenic radionuclides between the study area and the Flysch's soils could be mainly due to differences in the parent material that would explain slightly lower mean contents of ^{232}Th and ^{40}K in our soils. Likewise, the means of fallout radionuclides are also lower than in the Flysch's soils, supported by the fact that in our study site the mean annual precipitation is almost half than the recorded in the Pyrenean catchment (Navas et al., 2011).

Besides parent materials, a key factor in the environmental radioactivity levels is the particle size of soil, both because the fixation of fallout radionuclides in fine soil components and the association of lithogenic radionuclides to specific particle sizes. Thus, the concentration of clay minerals can affect the distribution of radionuclide bearing primary minerals and consequently radionuclide activity (Khater et al., 2013). In our soils the silt fraction dominates and as expected the PCA indicates that soil with high sand leads to lower adsorption of radionuclide to soil particles. The slightly lower content of the clay fraction in soils on limestones compared to siliciclastic ones is primarily related to differences in the composition of parent materials but another reason could be the significant leaching processes favoured by higher infiltration occurring in the karst parts of the catchment. This is further supported by higher values of hydraulic conductivity measured in soils developed on limestones in comparison to those recorded in soils on Keuper argillaceous materials (Gaspar et al., 2020b).

The topographic attributes have not an effect on the spatial distribution of the radionuclides. Apart from ^{137}Cs that was only weakly correlated with the slope gradient and altitude though this was an effect of the coincidence with better preserved soils under the natural plant cover on the higher altitude steep slopes.

The significant correlations between ^{137}Cs and $^{210}Pb_{ex}$ reflect their similar behaviour once they become attached to the fine soil fraction. However, the mass activities of lithogenic radionuclides are positively but not strongly correlated between them, which indicates a heterogeneous lithology and soils with different mineral components. The source of the lithogenic radionuclides in soils is the underlying bedrock thus previous studies in areas of very homogeneous lithology reported high correlations between lithogenic radionuclides (Fairbridge, 1972; Navas et al., 2011) while in our catchment the lithological differences result in lower correlations.

The close link of ^{232}Th and ^{40}K with soil minerals contained in the finer fraction of the soil is supported by their significant correlations with the content of clay. In turn, the lack of correlation between SOC and ^{40}K, and the low correlation between SOC and ^{232}Th further supports the association of these radionuclides with the soil mineral fraction.

Although radionuclides are known to have a very strong affinity for clay surface (Cornell, 1993; He and Walling, 1996; Forkapic et al., 2017) the relatively low content of the clay fraction and the limited range of variation in our soils (80% of the samples had clay content between 15% and 25%) might explain the lack of correlation found in the study soils. Our findings may lead to the assumption that the highly specific adsorption of radionuclides within the lattice structure of clays onto frayed edge sites (Brouwer et al., 1983) might be inhibited by the non-specific adsorption of fallout radionuclides in soils with high SOC content, which may be controlled by the high cationic exchange capacity of the organic matter.

The negative correlations between carbonate content and ^{137}Cs, ^{226}Ra, ^{232}Th and ^{40}K activities are likely because carbonate and bicarbonate anions can react with the radionuclides forming complexes that are either not adsorbed at all or only slightly adsorbed onto clays. The carbonate bearing cations, on the other hand, compete with the radionuclides for available adsorption sites. Our results agree with findings reported by other authors (Navas et al., 2005, 2011; Ahmad et al., 2019) and support the specific effect of the carbonate components of soil. Furthermore, the strong inverse correlations between SIC and mass activity of the lithogenic radionuclides might also be related to soil processes of carbonate leaching and subsequent precipitation that can be involved in their mobilization, especially in the case of ^{232}Th as it has also been reported by Cowart and Burnett (1994).

The absence of correlations of ^{238}U with the other radionuclides and soil properties suggests a totally different origin and behaviour and point to the relatively higher mobility of this radionuclide, which is consistent with findings of previous studies in carbonate rich soils (Navas et al., 2002a). The content of uranium in sedimentary rocks is highly variable and depends on the detrital source mineralogy. Thus, uranium can be present as a minor or trace component in a large number of other minerals, incorporated intrinsically by substitution of major ions within the crystal structure. In limestones, the trace concentration of uranium might be due to substitution in the lattice in the place of Ca^{2+} (Kabata-Pendias, 2011).

The models obtained to explain the variation of the radionuclides in soils on limestones and siliciclastic materials, respectively, illustrate the differences in the soil properties and the soil processes involved in the two types of lithologies. Models for the fallout radionuclides and ^{226}Ra included SOC as the main variable, supporting the evidence that these properties are strongly related, especially in soils on limestones. The

model for ^{137}Cs in limestones also included SIC accounting for the higher content of carbonates in these soils and its inverse relationship. However, the model for soils on siliciclastic materials include the silt fraction to explain part of the variance of ^{137}Cs what supports the relatively greater importance of the silt component in these soils. The absence of a correlation of ^{40}K with ^{238}U, ^{226}Ra and the fallout radionuclides reflects differences not only in its origin but in the soil processes and mobilization patterns. In reference to its origin, limestones contain only trace amounts of potassium, and it is essentially contained in the non-carbonate fraction, while in siliciclastic materials, the potassium content is largely controlled by the clay mineralogy (Wedepohl, 1978).

The different associations of soil properties and radionuclides in soils on limestones and siliciclastic materials are indicative of the different behaviour of the radionuclides. The association of the fine fractions, clay, and silt with ^{40}K, ^{232}Th, and ^{238}U (Fig. 3), confirm that the lithogenic radionuclides are contained in mineral lattices and their levels are controlled by the different mineral composition in limestones and siliciclastic materials. On the contrary, SOC appears related to ^{137}Cs and $^{210}Pb_{ex}$ because both incorporate in sediments after its fallout with wet and dry precipitations and are efficiently fixed by fine particles and organic carbon components in soils. In this regard, high affinity between $^{210}Pb_{ex}$ and organic matter was recorded in soil profiles along a transect on limestones (Gaspar et al., 2017). The content of SOC is the main explanatory factor for ^{137}Cs and $^{210}Pb_{ex}$. However, for ^{232}Th and ^{40}K, SOC is of much less importance and the carbonate content becomes the key factor controlling the inverse distribution of these two radionuclides.

490 *4.2 Spatial distribution of the radionuclides*

491 The different patterns of distribution of the radionuclides over the catchment are due
492 not only in relation to their different origins but because of the specific behaviour of the
493 fallout and lithogenic radionuclides. Based on the strong relationships found between the
494 fallout radionuclides and SOC, we can conclude that these radionuclides remain strongly
495 fixed to the organic matter, especially for ^{137}Cs.

496 The highest activities of ^{137}Cs and ^{210}Pb$_{ex}$ recorded in the northern third of the
497 catchment and the southwest area where the Mediterranean open forest and scrub areas
498 are more abundant are related with the strong direct relationships between the fallout
499 radionuclides and SOC, concluding that these radionuclides remain strongly fixed to the
500 organic matter, especially for ^{137}Cs. Hence, the content of SOC in soils is important to the
501 non-specific adsorption of fallout radionuclides in soils which is influenced by the cation
502 exchange capacity (CEC) of the organic matter, compared with the specific adsorption of
503 ^{137}Cs on clays (Rigol et al., 2002).

504 In the south part of the catchment, ^{210}Pb$_{ex}$ was most coincidental with the distribution
505 of the isolevels of SOC than ^{137}Cs, which might reflect a higher affinity between SOC
506 and ^{210}Pb$_{ex}$. This could be explained because most of the abandoned fields are
507 concentrated in this area, and the recovery of the natural vegetation may favour soil
508 protection against erosion, as recorded in a previous research in this area (Gaspar et al.,
509 2013). The activities of ^{210}Pb$_{ex}$, with continuous fallout, are more sensitive to the impact
510 of recent soil redistribution history. Thus, the different temporal window of this
511 radionuclide in relation to ^{137}Cs that will reflect more closely the processes occurring
512 during the last two decades is consistent with higher activities of ^{210}Pb$_{ex}$ in these sites.

513 The distinctive signature of ^{226}Ra in soils on limestones is because its link to materials
514 of carbonated origin (Kabata-Pendias, 2011), which in turn coincides with the occurrence

of more stony and organic soils. The concordance of the spatial distribution of ^{226}Ra and $^{210}Pb_{ex}$ is because the latter derives from the decay of gaseous ^{222}Rn, a daughter of ^{226}Ra (Joshi, 1987). Theoretically, ^{226}Ra and ^{210}Pb should be in secular equilibrium but owing to the diffusional behaviour of the noble gas daughter ^{222}Rn, dis-equilibrium can occur in natural materials (Ravichandran et al., 1995). In addition, the effect of water erosion inducing the mobilization of soil along with that of fine soil components bearing $^{210}Pb_{ex}$ introduces further discrepancies in the spatial distribution of ^{226}Ra and $^{210}Pb_{ex}$.

Most soils on limestones are covered by vegetation, which promotes the high content of SOC. Previous studies have shown that runoff and erosive processes are less intense on these soils, even on steep slopes (Gaspar et al., 2019). Hence, lesser strength of erosive processes could explain the higher activities of ^{137}Cs, $^{210}Pb_{ex}$ and ^{226}Ra in limestone soils that are better preserved and hold higher SOC content.

The low activities of ^{238}U in most soils on limestones are likely related to leaching processes favoured by their higher hydraulic conductivity in relation to much lower values recorded in argillaceous materials (Gaspar et al., 2020b). However, some high levels of ^{238}U in limestones at the northern part of the catchment in coincidence with high SOC content are likely because uranyl ions may be adsorbed or form organic-metallic species with organic matter, hosting significant high concentrations in organic-rich soils (Kabata-Pendias, 2011). Furthermore, Sheppard and Evenden (1988) indicate that uranium mobility increases by the presence of carbonate, through the formation of anionic U and CO_3 complexes. The high isolevels of ^{238}U in soils on siliciclastic materials is likely because these soils might retain more uranium as it appears frequently associated with clays due to the affinity of the clay fraction for absorbing U (Megumi and Mamuro, 1977).

Along the soil transects, the variation of the radionuclides activities showing paralleled patterns to SOC but opposite to SIC, appears to be influenced by some soil

properties. The siliciclastic section of transect a-a' and b-b' shows an increase in ^{232}Th, ^{40}K and ^{226}Ra at the bottom part, which could reflect the mobilisation and accumulation of these radionuclides with soil. The opposite pattern is observed for transect c-c', with depletion of radionuclides at the end of the transect, which is in coincidence with eroded areas. The trend is less clear for transect d-d', which is located in a more stable area in terms of redistribution processes. If we compare the distribution maps of the radionuclides with the soil redistribution maps (Navas et al., 2013, 2014) we can observe a depletion of ^{232}Th, ^{40}K and ^{226}Ra in some areas located in the northern and northwest of the catchment, where soil loss is more intense. Despite not finding these coincidences in other areas of the catchment, where erosion processes are less intense, we can conclude that soil redistribution processes affect the mobilization of ^{232}Th, ^{40}K and ^{226}Ra.

In general, there is a general depletion of fallout radionuclides and of ^{226}Ra and ^{232}Th in soils with low-permeability on siliciclastic materials of the cultivated lowlands that experience increased runoff and soil transport capacity thus intensifying water erosion as recorded by Gaspar et al. (2020b). Greater soil erosion triggers the mobilization of the radionuclides together with the fine soil particles as it was observed for some trace elements along a slope transect in the study area (Gaspar et al., 2020a). In turn, the enrichment of ^{238}U and ^{40}K in some parts surrounding the lakes might be due to deposition of fine particles in the gentle slope lowlands.

5. Conclusions

Our study provides a holistic picture of the content and distribution of fallout and lithogenic radionuclides in a complex mountain agroforestry system. We can conclude that the specific activity of most of the radionuclides differs according to the parent material, apart from ^{238}U. The differences of lithology along with the distinctive soil

properties explain a major part of the radionuclides variation. Soils on limestones recorded higher activities of ^{226}Ra as well as of fallout radionuclides, the latter linked to high SOC content. However, in soils on siliciclastic materials the higher activities of ^{40}K and ^{232}Th, that are correlated with the clay fraction but have low correlations with SOC, support the affinity of these radionuclides with the fine soil fractions. ^{238}U had a totally different behaviour as demonstrated by the lack of correlations with soil properties or any model to explain the ^{238}U variance and exhibited distinctive distribution patterns controlled by a variety of soil processes affecting its mobility.

The effect of soil redistribution processes increased the percentage of explanation of the total variation for most radionuclides, especially for ^{137}Cs. The fact that coincidences were found between the spatial distribution of soil loss and soil deposition with the depletion and enrichment of radionuclides in some areas of the catchment where these processes are more intense, confirms the effect of the lateral mobilisation of ^{137}Cs, $^{210}Pb_{ex}$, ^{226}Ra, ^{232}Th and ^{40}K by soil redistribution processes. The trends of the radionuclides with the distance along the selected transects also reinforce the impact of water erosion on their mobilisation. The more distinct spatial distribution of uranium is likely due to differential processes of leaching and water erosion occurring in soil on limestones and siliciclastic materials across the catchment. Our findings contribute to a more comprehensive knowledge of the main drivers affecting the radionuclides patterns in a representative Mediterranean landscape, concluding that differences between parent materials in areas of sedimentary rocks lead to different spatial distribution of lithogenic and fallout radionuclides.

590 **Acknowledgment**

591 This research has been supported by projects PID2019-104857RB-I00 and PID2019-
592 103946RJ-I00 funded by the Spanish Ministry of Science and Innovation (State Research
593 Agency).

594

595 **References**

596 Ahmad, A.Y., Al-Ghouti, M.A., AlSadig, I., Abu-Dieyeh, M., 2019. Vertical distribution
597 and radiological risk assessment of ^{137}Cs and natural radionuclides in soil samples.
598 Scientific Reports 9, 12196.

599 Brouwer, E., Baeyens, B., Maes, A., Cremers, A., 1983. Cesium and rubidium ion
600 equilibriums in illite clay. J. Phys. Chem. 87, 1213–1219.

601 Cornell, R.M., 1993. Adsorption of cesium on minerals: a review. J Radioanal Nucl
602 Chem. 171, 483–500.

603 Cowart, J.B., Burnett, W.C., 1994. The Distribution of Uranium and Thorium Decay-
604 Series Radionuclides in the Environment - A Review. J. Environ. Qual. 23, 651–662.

605 De Jong, E., Acton, D.F., Kozak, L.M., 1994. Naturally occurring gamma-emitting
606 isotopes, radon release and properties of parent materials of Saskatchewan soils. Can.
607 J. Soil Sci. 74, 47–53.

608 Elless, M.P., Lee, S.Y., 2002. Radionuclide-contaminated soils: A mineralogical
609 perspective fortheir remediation. In: Soil Mineralogy with Environmental
610 Applications, SSSA Book Series, no. 7, 37–763. (J. Dixon and D. Schulze, eds.), Soil
611 Science Society of America, Madison,WI.

612 Fairbridge, R.W., 1972. The encyclopaedia of geochemistry and environmental sciences.
613 Vol. 4A. pp. 1215-1228. Van Nostrand Reinhold Co., New York, NY.

Forkapic, S. Vasin, J., Bikit, I., Mrdja, D., Bikit, K., Milić, S., 2017. Correlations between soil characteristics and radioactivity content of Vojvodina soil. J. Environ. Radioact. 166, 104–111.

Gaspar, L., Navas, A., 2013. Vertical and lateral distributions of ^{137}Cs in cultivated and uncultivated soils on Mediterranean hillslopes. Geoderma 207-208, 131–143.

Gaspar, L., Navas, A., Walling, D.E., Machín, J., Gómez-Arozamena, J., 2013. Using ^{137}Cs and $^{210}Pb_{ex}$ to assess soil redistribution on slopes at different temporal scales. Catena 102, 46–54.

Gaspar, L., Webster, R., Navas, A., 2017. Fate of $^{210}Pb_{ex}$ fallout in soil under forest and scrub of the central Spanish Pre-Pyrenees. European Journal of Soil Science 68, 259–269.

Gaspar, L., Quijano, L., Lizaga, I., Navas, A., 2019. Effects of land use on soil organic and inorganic C and N at ^{137}Cs traced erosional and depositional sites in mountain agroecosystems. Catena 181, 104058.

Gaspar, L., Lizaga, I., Navas, A., 2020a. Elemental mobilisation by sheet erosion affected by soil organic carbon and water fluxes along a radiotraced soil catena with two contrasting parent materials. Geomorphology 370, 107387.

Gaspar, L., Mabit, L., Lizaga, I., Navas, A., 2020b. Lateral mobilization of soil carbon induced by runoff along karstic slopes. J Environ Manage 260, 110091.

Graham, E.R. 1964. Radioisotopes and soils. In: F.E. Bear, ed. Chemistry of the soil. pp. 445-473. Van Nostrand Reinhold Co., New York, NY.

He, Q., Walling, D.E., 1996. Interpreting the particle size effect in the adsorption of Cesio-137 and unsupported Pb-210 by mineral soils and sediments. J. Environ. Qual. 13, 301–304.

638 Iurian, A.R., Phaneuf, M.O., Mabit, L., 2015. Mobility and bioavailability of
639 radionuclides in soils. In: Walther C, Gupta KD, editors. Radionuclides in the
640 Environment: Influence of Chemical Speciation and Plant Uptake on Radionuclide
641 Migration. Cham: Springer International Publishing; pp. 37–59.
642 Joshi, S.R., 1987. Non-destructive determination of lead-210 and radium-226 in
643 sediments by direct photon analysis. J. Radioanal. Nucl. Chem.116, 169–182.
644 Kabata-Pendias, A., 2011. Trace elements in soils and plants. 4rd 684 ed. CRC Press. Boca
645 Raton, Fla. 505 p.
646 Khater, A.E.M., Al-Mobark, L.H., Aly, A.A., Al-Omran, A.M., 2013. Natural
647 radionuclides in clay deposits: Concentration and dose assessment. Radiation
648 Protection Dosimetry 156(3), 321–330.
649 Lal, R., 2003. Soil erosion and the global carbon budget. Environment International 29(4),
650 437–450.
651 Lizaga, I., Gaspar, L., Latorre, B., Navas, A., 2020. Variations in transport of suspended
652 sediment and associated elements induced by rainfall and agricultural cycle in a
653 Mediterranean agroforestry catchment. Journal of Environmental Management 272,
654 111020.
655 Mabit, L., Benmansour, M., Walling, D.E., 2008. Comparative advantages and
656 limitations of the fallout radionuclides ^{137}Cs, $^{210}Pb_{ex}$ and ^{7}Be for assessing soil
657 erosion and sedimentation. J. Environ. Radioactiv. 99(12), 1799–1807.
658 Mabit, L., Bernard, C., Lee Zhi Yi, A., Fulajtar, E., Dercon, G., Zaman, M., Toloza, A.,
659 Heng, L., 2018. Promoting the use of isotopic techniques to combat soil erosion: An
660 overview of the key role played by the SWMCN Subprogramme of the Joint
661 FAO/IAEA Division over the last 20 yr. Land Degrad Dev. 29, 3077–3091.

662 Megumi, K., Mamuro, T., 1977. Concentration of uranium series nuclides in soil particles
663 in relation to their size. J. Geophys. Res. 82, 353–356.
664 Motha, J.A., Wallbrink, P.J., Hairsine, P.B., Grayson, R.B., 2003. Determining the
665 sources of suspended sediment in a forested catchment in southeaster Australia.
666 Water Resour. Res. 39, 1056.
667 Navas, A., Soto, J., Machín, J., 2002a. Edaphic and physiographic factors affecting the
668 distribution of natural gamma-emitting radionuclides in the soils of the Arnás
669 catchment in the Central Spanish Pyrenees. European Journal of Soil Science 53,
670 629–638.
671 Navas, A., Soto, J., Machín, J., 2002b. ^{238}U, ^{226}Ra, ^{210}Pb, ^{232}Th and ^{40}K activities in soil
672 profiles of the Flysch sector (Central Spanish Pyrenees). Applied Radiation and
673 Isotopes 57(4), 579–589.
674 Navas, A., Machín, J., Soto, J., 2005. Mobility of natural radionuclides and selected major
675 and trace elements along soil toposequence in the central Spanish Pyrenees. Soil Sci.
676 170(9), 743–757.
677 Navas, A., Gaspar, L., López-Vicente, M., Machín, J., 2011. Spatial distribution of
678 natural and artificial radionuclides at the catchment scale (South Central Pyrenees).
679 Radiat. Meas. 46(2), 261–269.
680 Navas, A., López-Vicente, M., Gaspar, L., Machín, J., 2013. Assessing soil redistribution
681 in a complex karst catchment using fallout ^{137}Cs and GIS. Geomorphology 196, 231–
682 241.
683 Navas, A., López-Vicente, M., Gaspar, L., Palazón, L., Quijano, L., 2014. Establishing a
684 tracer-based sediment budget to preserve wetlands in Mediterranean mountain
685 agroecosystems (NE Spain). Sci. Total Environ. 496, 132–143.

686 Navas, A., Lizaga, A., Gaspar, L., Latorre, B., Dercon, G., 2020. Unveiling the
687 provenance of sediments in the moraine complex of Aldegonda Glacier (Svalbard)
688 after glacial retreat using radionuclides and elemental fingerprints. Geomorphology
689 367, 107304.
690 Owens, P.N., Blake, W.H., Gaspar, L., Gateuille, D., Koiter, A.J., Lobb, D.A., Petticrew,
691 E.L., Reiffarth, D.G., Smith H.G., Woodward, J.C., 2016. Fingerprinting and tracing
692 the sources of soils and sediments: Earth and ocean science, geoarchaeological,
693 forensic, and human health applications. Earth-Science Reviews 162, 1–23.
694 Palazón, L., Latorre, B., Gaspar, L., Blake, W.H., Smith, H.G., Navas, A., 2015.
695 Comparing catchment sediment fingerprinting procedures using an auto-evaluation
696 approach with virtual sample mixtures. Sci. Total Environ. 532, 456–466.
697 Ravichandran, M., Baskaran, M., Santschi, P.H., Bianchi, T.S., 1995. Geochronology of
698 sediments in the Sabine-Neches estuary, Texas, USA. Chem Geol 125, 291–306.
699 Rigol, A., Vidal, M., Rauret, G., 2002. An overview of the effect of organic matter on
700 soil–radiocaesium interaction: implications in root uptake. Journal of Environmental
701 Radioactivity 58(2–3), 191–216.
702 Ritchie, J.C., McHenry, J.R., 1990. Application of radioactive fallout ^{137}Cs for measuring
703 soil erosion and sediment accumulation rates and patterns: a review Journal of
704 Environmental Quality 19, 215–233.
705 Shender, M.A., 1997. Measurement of natural radioactivity levels in soil in Tripoli. Appl.
706 Radiat. Isot. 48, 147–8.
707 Sheppard, S.C., Evenden, W.G., 1988. Critical compilation and review of plant/soil
708 concentration ratios for uranium, thorium and lead. J. Environ. Radioactivity 8, 255-
709 285.

Smičiklas, I., Jović, M., Šljivić-Ivanović, M., Mrvić, V., čakmak, D., Dimović, S., 2015. Correlation of Sr^{2+} retention and distribution with properties of different soil types. Geoderma 253–254, 21–29.

Soto, J., Navas, A., 2004. A model of ^{137}Cs activity profile for soil erosion studies in uncultivated soils of Mediterranean environments. J. Arid Environ. 59, 719–730.

Soto, J., Navas, A., 2008. A simple model of Cs-137 profile to estimate soil redistribution in cultivated stony soils. Radiat. Meas. 43, 1285–1293.

Sposito, G., 2008. The Chemistry of Soils. 2nd edition. New York: Oxford University Press. 330 p.

UNSCEAR (United Nations Scientific Committee of the Effect of Atomic Radiation) 2000 Sources, Effects and Risks Ionizing Radiations (New York: United Nations).

Van Cleef, D.J., 1994. Determination of ^{226}Ra in soil using ^{214}Pb and ^{214}Bi immediately after sampling. Health Phys. 67, 288–289.

Walling, D.E., 2012. Fallout radionuclides and the study of erosion and sedimentation R.A. Meyers (Ed.), Encyclopedia of Sustainability Science and Technology, Springer. 3705-3768.

Wedepohl, K.H., 1978. Handbook of Geochemistry: Volume II/2 Elements Si(14) to V(23). Springer-Verlag, Berlin, Heidleberg & New York.

Yao, S.C., Xue, X., 2016. Sediment records of the metal pollution at Chihu Lake near a copper mine at the middle Yangtze River in China. Journal of Limnology 75, 121–134.

Figures

Fig. 1 Location of the study catchment (Estaña, NE Spain). i) Geological map (IGME), ii) soil redistribution data (produced based on data from Navas et al., 2013, 2014), iii) Grid distribution of 228 soil samples on limestones (Muschelkalk facies) and siliciclastic materials (Keuper facies and Quaternary deposits), and the four selected transects.

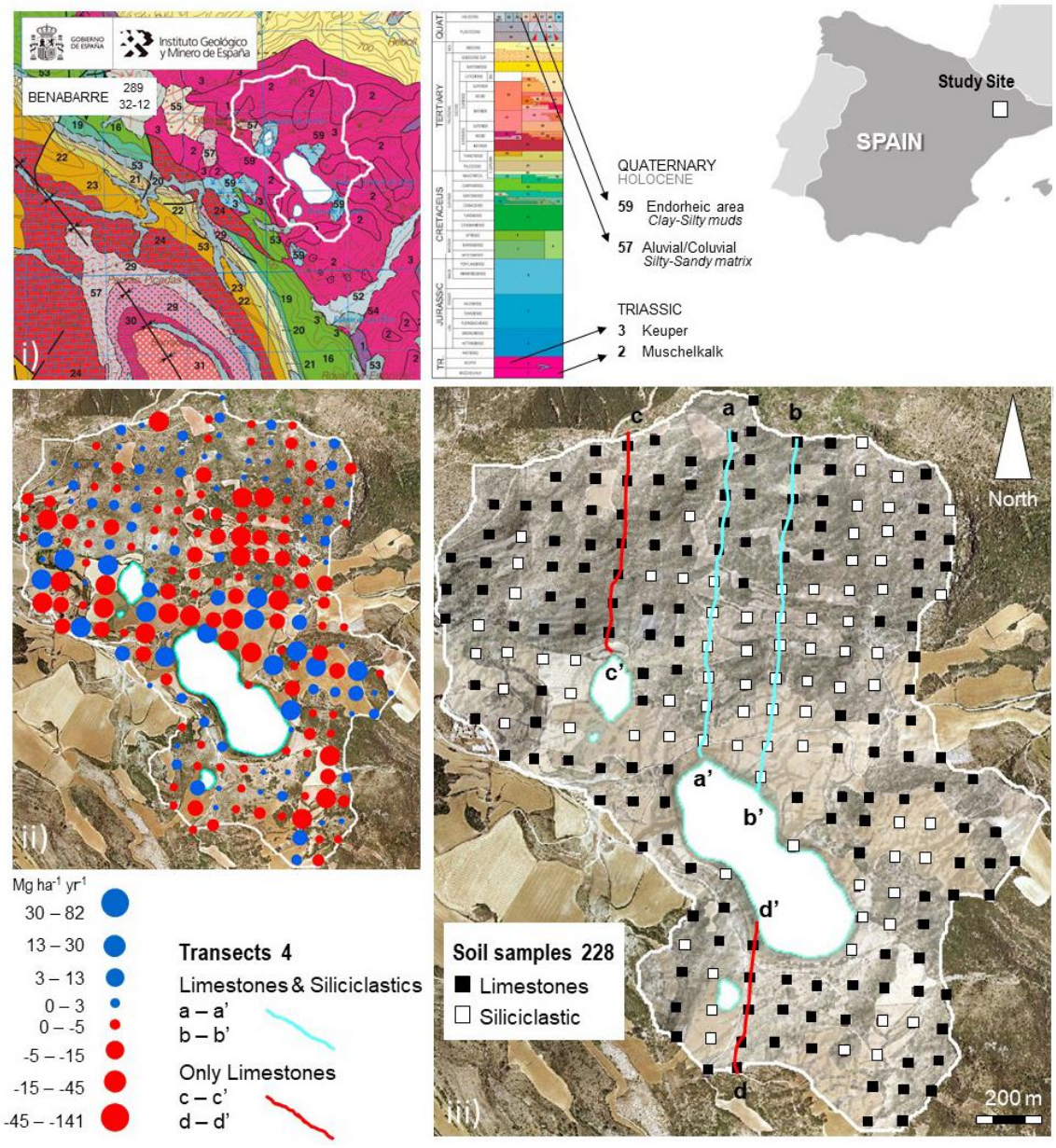

Fig 2. 2D scatter plot diagram of discriminant function analysis (DFA) including fallout and lithogenic radionuclides and the main soil properties.

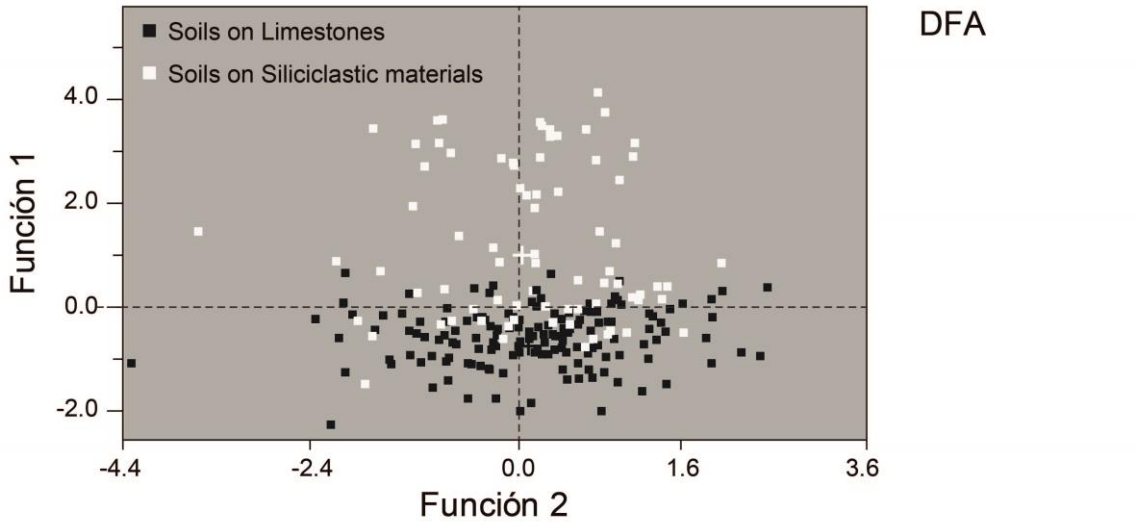

Fig 3. Biplot diagram of the principal component analysis (PCA) based on the two main components showing vectors of fallout and lithogenic radionuclides and the main soil properties.

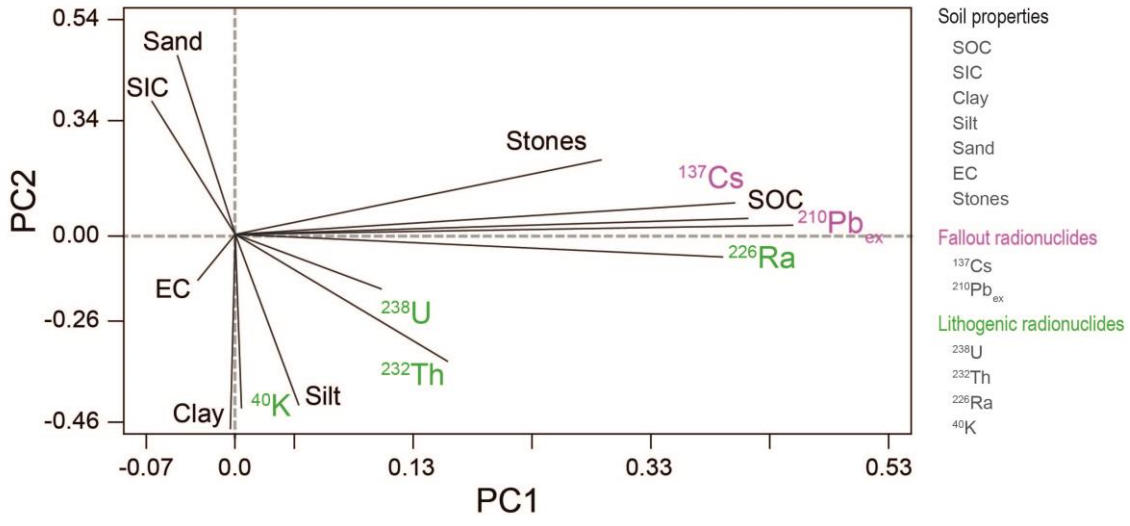

Fig 4. Spatial distribution of fallout radionuclides mass activities (Bq kg^{-1}) across the study catchment and overlay of the isolevels of SOC, SIC and clay contents (%).

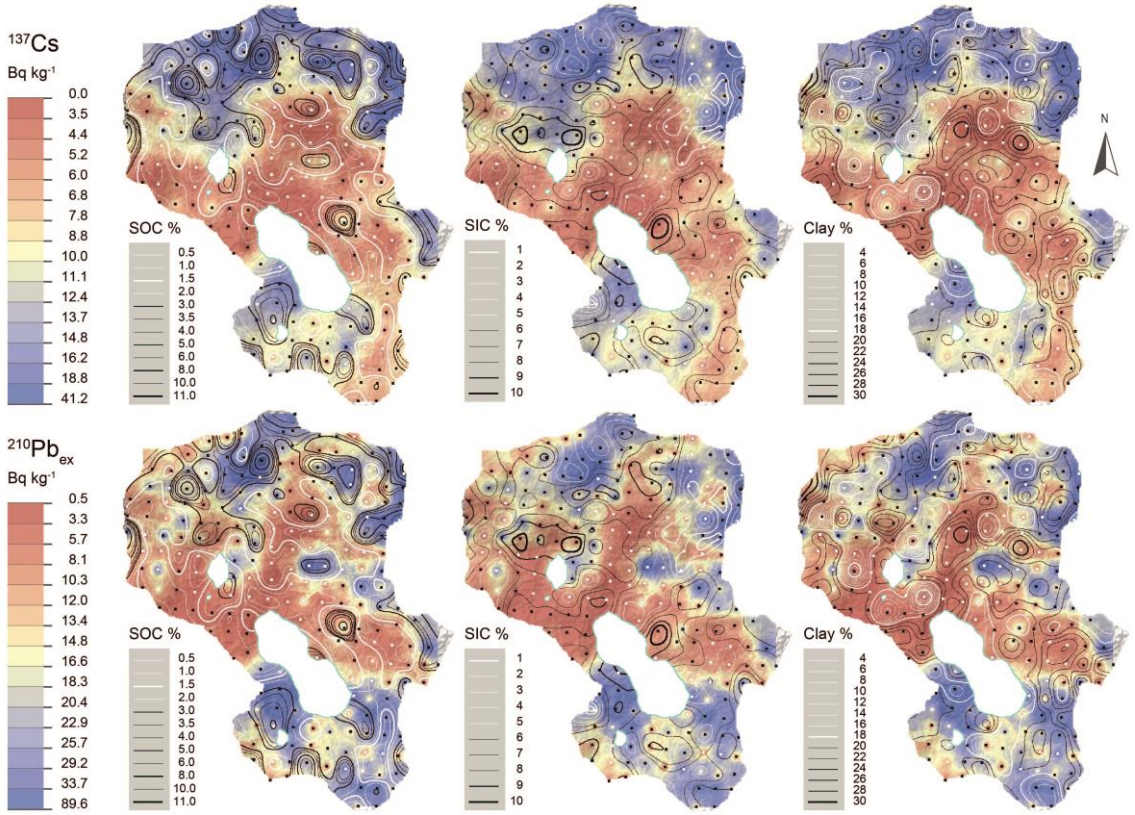

Fig 5. Spatial distribution of lithogenic radionuclides mass activities (Bq kg^{-1}) across the study catchment and overlay of the isolevels of SOC, SIC and clay contents (%).

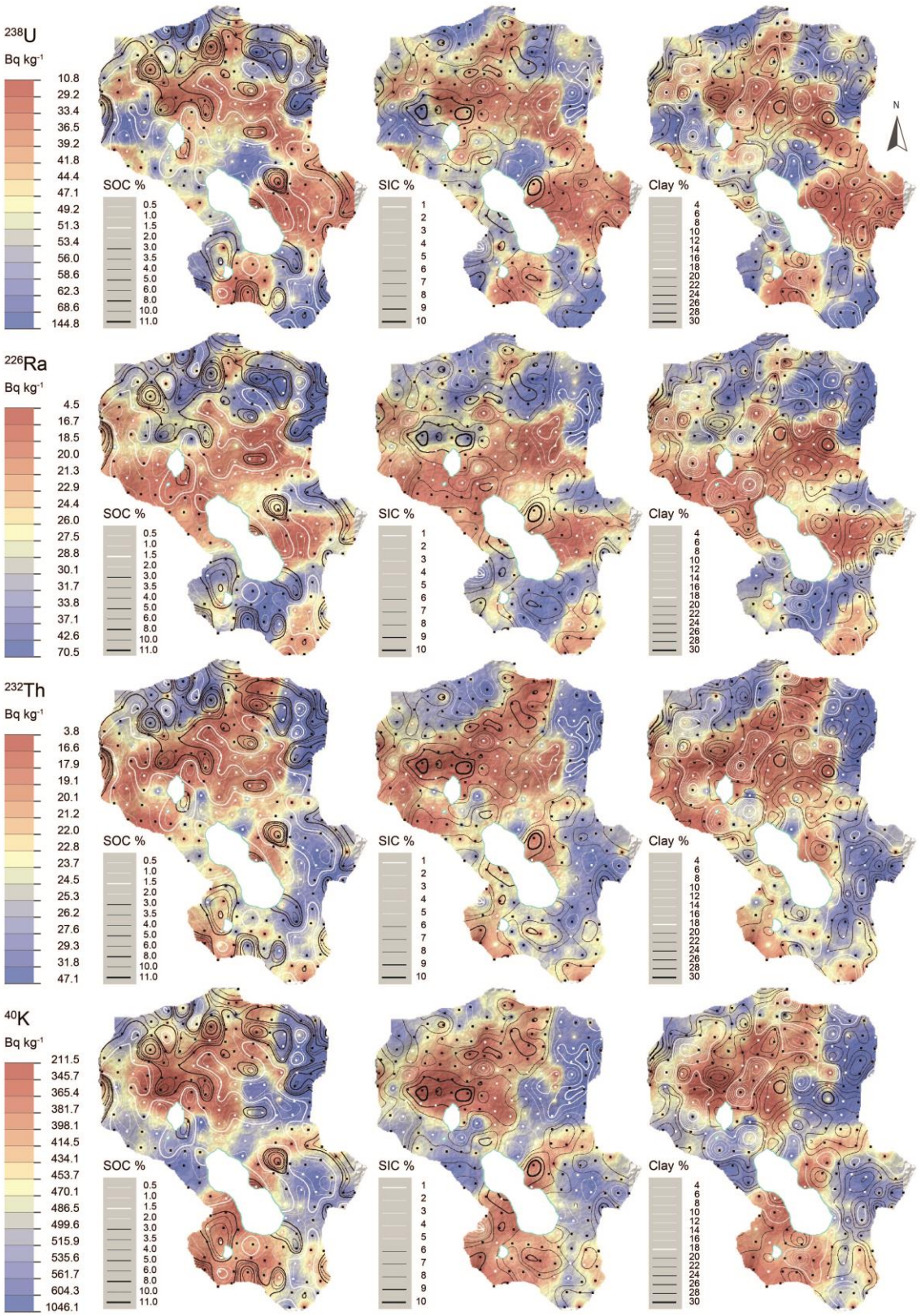

761 **Fig 6**. Soil properties, fallout and lithogenic radionuclides along the four selected

762 transects, from the upper (x) to the bottom (x') slope.

763 *Dotted lines show the linear trendline along the transects*

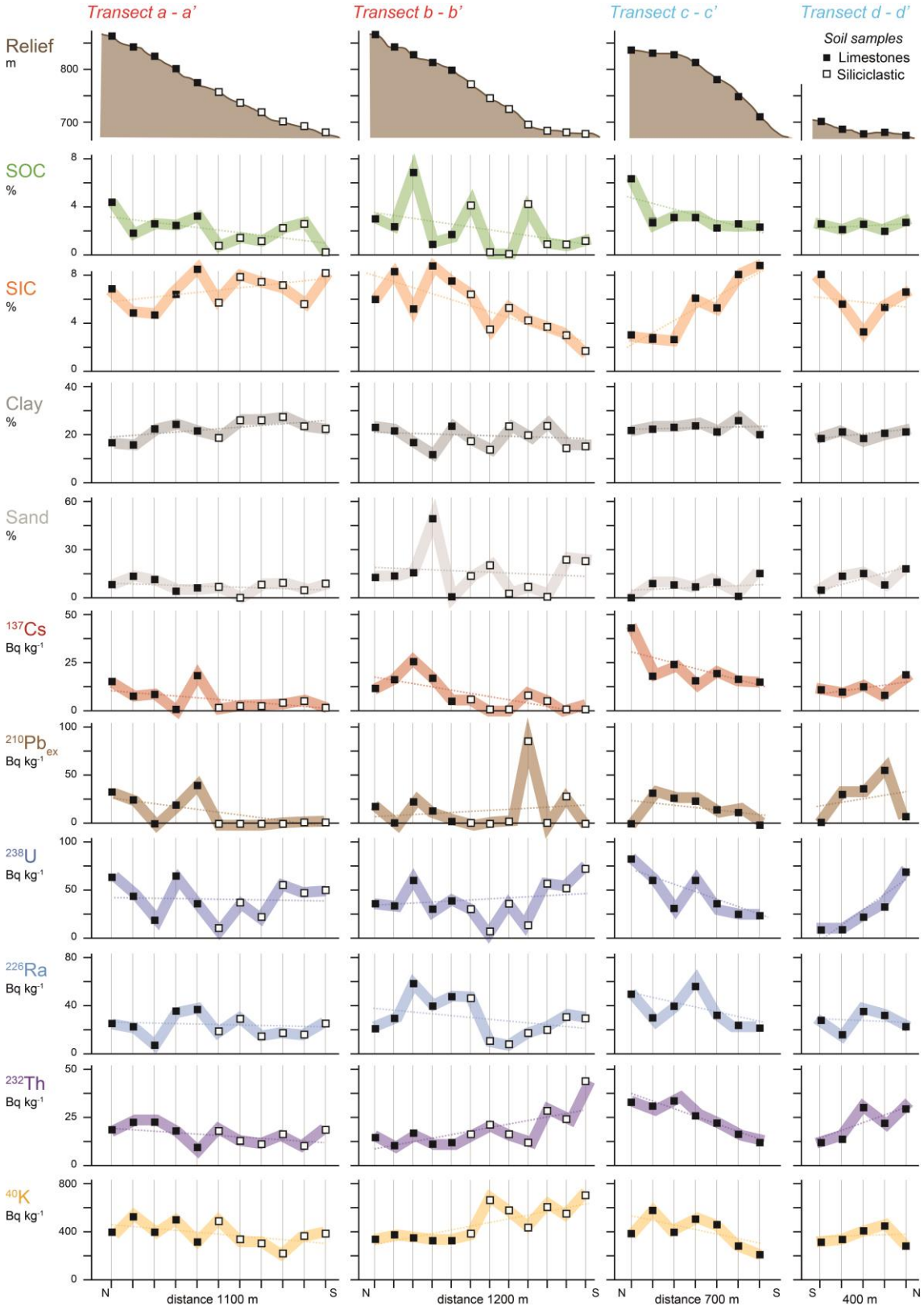

764

765 **Table 1.** Basic statistics for the mass activity of fallout and lithogenic radionuclides (Bq
766 kg^{-1}) and the main soil properties analysed in the soil samples.
767

		Mean	SD	Min.	Max.
Fallout radionuclides					
^{137}Cs	Bq kg^{-1}	10.2	8.3	0.4	43.8
$^{210}Pb_{ex}$	"	17.2	20.3	0.5	101.8
Lithogenic radionuclides					
^{238}U	Bq kg^{-1}	48.1	23.9	10.0	146.0
^{226}Ra	"	27.9	14.3	2.0	73.0
^{232}Th	"	23.4	8.8	2.0	50.0
^{40}K	"	464.2	150.1	155.0	1080.0
Soil properties					
SOC	%	2.48	1.94	0.07	11.06
SIC	"	5.03	2.16	0.42	10.30
$CaCO_3^=$	"	41.91	18.03	3.48	85.81
Stones	"	29.02	15.50	0.00	76.18
Sand	"	10.28	13.06	0.00	80.93
Silt	"	67.71	10.12	15.50	79.96
Clay	"	21.79	4.70	3.57	31.79
EC	dSm^{-1}	0.55	0.62	0.11	2.32

768
769

770 **Table 2.** ANOVA and Kruskal-Wallis analysis for the mass activity of fallout and
771 lithogenic radionuclides (Bq kg^{-1}) and the main soil properties by different groups of
772 parent material. Asterisks indicate significant differences between soils on limestones and
773 siliciclastic rocks (**Anova test*, *** Kruskal-Wallis test*).
774

		Soils on Limestones			Soils on Siliciclastic materials				ANOVA	KW
		Median	Mean	SD	Median	Mean	SD		p-value	p-value
Fallout radionuclides										
^{137}Cs	Bq kg^{-1}	10.5	11.8	8.5	5.2	7.1	7.0	*	**0.000**	**0.000**
$^{210}Pb_{ex}$	"	14.6	18.9	20.1	4.4	14.1	20.5	**	0.091	**0.026**
Lithogenic radionuclides										
^{238}U	Bq kg^{-1}	47.5	49.0	23.8	43.5	46.4	24.3		0.448	0.358
^{226}Ra	"	29.5	31.1	14.4	19.0	21.8	12.1	*	**0.000**	**0.000**
^{232}Th	"	23.2	23.3	8.9	22.0	23.5	8.8		0.878	0.954
^{40}K	"	430.0	449.4	140.2	462.5	492.6	164.7	*	**0.039**	**0.037**
Soil properties										
SOC	%	2.49	2.72	1.94	1.17	2.02	1.87	*	**0.009**	**0.000**
SIC	"	5.60	5.50	2.00	4.11	4.13	2.20	*	0.000	0.000
$CaCO_3^=$	"	46.69	45.83	16.63	34.24	34.39	18.31	*	**0.000**	**0.000**
Stones	"	31.65	32.52	14.22	18.36	22.29	15.73	*	**0.000**	**0.000**
Sand	"	8.20	10.90	12.19	4.97	9.09	14.60	**	0.322	**0.005**
Silt	"	68.84	67.47	8.96	71.60	68.17	12.09	**	0.621	**0.019**
Clay	"	21.3	20.63	4.50	22.87	22.10	5.09		0.472	0.203
EC	dSm^{-1}	0.27	0.30	0.12	0.55	1.04	0.85	*	**0.000**	**0.000**

775
776

777 **Table 3**. Pearson correlation coefficients between radionuclides (Bq kg^{-1}) and main soil
778 properties in the soils of the catchment. *Bold numbers indicate statistical significance at*
779 *$p \leq 0.05$ level. Dark blue (1, 0.5), blue (0.5, 0.1), white (0.1, -0.1), red (-0.1, -0.5), dark*
780 *red (-0.5, -1).*
781

		SOC %	SIC %	Stones %	Sand %	Silt %	Clay %	EC dSm^{-1}
Soils on Limestones								
^{137}Cs	*Bq kg^{-1}*	**0.71**	**-0.28**	**0.36**	0.01	0.00	-0.03	**0.37**
$^{210}Pb_{ex}$	"	**0.36**	-0.11	**0.19**	-0.08	0.11	0.00	**0.32**
^{238}U	"	0.03	-0.08	0.04	-0.10	0.11	0.05	0.01
^{226}Ra	"	**0.41**	**-0.27**	**0.33**	-0.07	0.07	0.07	0.16
^{232}Th	"	**0.23**	**-0.70**	**-0.19**	**-0.17**	0.10	**0.26**	0.04
^{40}K	"	-0.04	**-0.65**	**-0.39**	**-0.22**	0.11	**0.38**	-0.14
Soils on Siliciclastic materials								
^{137}Cs	*Bq kg^{-1}*	**0.79**	0.13	**0.63**	-0.19	0.09	-0.14	0.00
$^{210}Pb_{ex}$	"	**0.58**	-0.12	**0.24**	-0.15	0.04	-0.08	**0.30**
^{238}U	"	0.09	-0.01	0.11	0.12	-0.14	0.12	0.03
^{226}Ra	"	**0.61**	-0.03	**0.57**	0.00	-0.11	0.04	-0.08
^{232}Th	"	**0.15**	**-0.34**	0.04	0.07	-0.14	0.09	-0.16
^{40}K	"	-0.09	**-0.52**	**-0.32**	0.13	-0.17	0.14	-0.08

782
783

784 **Table 4**. Step-wise multiple regression analysis of the relationship between each
785 radionuclide and the main soil properties for limestone and siliciclastic soils.
786

	Step	Overall soils			Soils on Limestones			Soils on Siliciclastic materials		
		Variable	R^2	P	Variable	R^2	P	Variable	R^2	P
^{137}Cs										
	1st	SOC	54.2	0.000	SOC	50.0	0.000	SOC	62.0	0.000
	2nd	Stones	57.8	0.000	Stones	51.5	0.001	Stones	68.4	0.000
	3rd	Silt	58.8	0.020	SIC	53.1	0.027	Silt	70.7	0.020
	4th									
$^{210}Pb_{ex}$										
	1st	SOC	19.4	0.000	SOC	13.0	0.003	SOC	33.8	0.000
	2nd	EC	21.8	0.016	EC	15.9	0.028	EC	44.4	0.001
	3rd									
	4th									
^{226}Ra										
	1st	SOC	24.0	0.000	SOC	17.1	0.007	SOC	37.0	0.001
	2nd	Stones	31.9	0.000	Stones	21.0	0.001	Stones	45.6	0.000
	3rd	SIC	35.0	0.000	SIC	27.0	0.000	SIC	51.1	0.005
	4th	EC	37.7	0.002						
^{232}Th										
	1st	SIC	29.9	0.000	SIC	49.2	0.000	SIC	11.5	0.000
	2nd	EC	40.7	0.000				EC	25.9	0.000
	3rd	SOC	41.8	0.040				Stones	31.1	0.021
	4th									
^{40}K										
	1st	SIC	36.5	0.000	SIC	42.1	0.000	SIC	26.7	0.000
	2nd	EC	43.3	0.000	Stones	49.2	0.000	EC	42.0	0.000
	3rd	Stones	48.1	0.000	EC	53.6	0.000			
	4th	Clay	49.5	0.011	Clay	56.7	0.002			

787